UNIVERSITI MALAYSIA PAHANG

BORANG PENGESAHAN STATUS TESIS

JUDUL : COMPUTATIONAL FLUID DYNAMICS (CFD) OF ADVANCED GAS DISPERSION: DEEP HOLLOW BLADE TURBINE

SESI PENGAJIAN : 2011/2012

Saya **NORLEEN BT ISA**
(HURUF BESAR)

mengaku membenarkan tesis (PSM/~~Sarjana~~/~~Doktor Falsafah~~)* ini disimpan di Perpustakaan Universiti Malaysia Pahang dengan syarat-syarat kegunaan seperti berikut :

1. Tesis adalah hakmilik Universiti Malaysia Pahang
2. Perpustakaan Universiti Malaysia Pahang dibenarkan membuat salinan untuk tujuan pengajian sahaja.
3. Perpustakaan dibenarkan membuat salinan tesis ini sebagai bahan pertukaran antara institusi pengajian tinggi.
4. **Sila tandakan (√)

[ ] SULIT (Mengandungi maklumat yang berdarjah keselamatan atau kepentingan Malaysia seperti yang termaktub di dalam AKTA RAHSIA RASMI 1972)

[ ] TERHAD (Mengandungi maklumat TERHAD yang telah ditentukan oleh organisasi/badan di mana penyelidikan dijalankan)

[√] TIDAK TERHAD

Disahkan oleh

(TANDATANGAN PENULIS) (TANDATANGAN PENYELIA)

Alamat Tetap: 23,Selasar Loke Lim,
Loke Lim Garden,
30010 Ipoh,
Perak Darul Ridzuan

DR. JOLIUS GIMBUN
Nama Penyelia

Tarikh:January 2012 Tarikh: January 2012

CATATAN: * Potong yang tidak berkenaan.
** Jika tesis ini **SULIT** atau **TERHAD**, sila lampirkan surat daripada pihak berkuasa/organisasiberkenaan dengan menyatakan sekali sebab dan tempoh tesis ini perlu dikelaskan sebagai **SULIT** atau **TERHAD**.
♦ Tesis dimaksudkan sebagai tesis bagi Ijazah Doktor Falsafah dan Sarjana secara penyelidikan, atau disertasi bagi pengajian secara kerja kursus dan penyelidikan, atau Lapuran Projek Sarjana Muda (PSM).

SUPERVISOR'S DECLARATION

"I hereby declare that I have read this thesis and in my opinion this thesis has fulfilled the qualities and requirements for the award of Bachelor of Engineering (Chemical)"

Signature : ....

Name of Supervisor : Dr. Jolius Gimbun

Date : ………………………

STUDENT'S DECLARATION

"I hereby declared that the work in this thesis is my own except for quotations and summaries which have been duly acknowledged. The thesis has not been accepted for any degree and is not concurently submitted in candidature of any other degree."

Signature :..........................

Name : Norleen bt Isa

Date : 13 January 2012

COMPUTATIONAL FLUID DYNAMICS OF ADVANCED GAS DISPERSION: DEEP HOLLOW BLADE TURBINE

NORLEEN BT ISA

A thesis submitted in fulfillment of the

requirements for the award of the degree of

Bachelor of Chemical Engineering

Faculty of Chemical Engineering

UNIVERSITI MALAYSIA PAHANG

JANUARY 2012

To my beloved family

ACKNOWLEDGEMENT

This research would not have been possible without the guidance and help of several individuals who in one way or another contributed and extended their valuable assistance in the preparation and completion of this research. First and foremost, my outmost gratitude to Dr Jolius Gimbun, my supervisor whose through invaluable guidance and constant supervision as well as sacrificing time and providing necessary information regarding my research.

I am highly indebted towards my colleagues for their kind co-operation and encouragement which help me in completion of this research. My thanks and appreciations also go to all technical staffs and people who have willingly helped me out with their abilities.

Last but not the least, my family for their love and the one above all of us, praise is to Allah for answering my prayers, for giving me strength and guidance until this undergraduate research project is complete.

ABSTRACT

Stirred tanks are widely used in the chemical and biochemical process industries. Mixing, fermentation, polymerization, crystallization and liquid-liquid extractions are significant examples of industrial operations usually carried out in tanks agitated by one or more impellers. The flow phenomena inside the tank are of great importance in the design, scale-up and optimization of tasks performed by stirred tanks. This work presents of a stirred tank agitated by an advanced gas dispersion impeller namely deep hollow blade turbine (HEDT) using Computational Fluid Dynamic (CFD) method. The standard k-ε, realizable k-ε and shear-stress transport k-ϖ were considered in this study for comparison purposes. Predictions of the impeller-angle-resolved and time-averaged turbulent flow have been evaluated and compared with data from Particle Image Velocimetry (PIV) measurements. Multiple Reference Frame (MRF) used to capture flow features in details and predicts flow for steady state for the impeller blades relative to the tank baffles. Unsteady solver indeed predicts periodic shedding, and leads to much better concurrence with available experimental data than has been achieve with steady computation.

ABSTRAK

Tangki pengacau digunakan secara meluas dalam industri pemprosesan kimia dan biokimia. Proses pengacauan, penapaian, pempolimeran, penghabluran dan pengekstrakan cecair adalah contoh ketara operasi di dalam industri yang biasanya dilakukan di dalam tangki pengacau menggunakan satu *impeller* atau lebih. Fenomena aliran di dalam tangki amat penting dalam proses mereka bentuk, meningkatkan skala dan optimumkan prestasi tanki pengacau. Kajian ini membentangkan tangki pengacau menggunakan *impeller* terkini untuk sebaran gas yang maju iaitu *deep hollow blade turbine* (HEDT) menggunakan kaedah *Computational Fluid Dynamic* (CFD). *Standard k-ε, realizable k-ε* dan *shear-stress transport k-ω* dipertimbangkan untuk tujuan perbandingan kajian ini. Ramalan *impeller-angle resolve* dan aliran *turbulent* berdasarkan masa telah dinilai dan dibandingkan dengan data yang diukur menggunakan kaedah *Particle Image Velocimetry* (PIV). *Multiple Reference Frame* (MRF) digunakan untuk mengetahui ciri-ciri aliran dengan terperinci dan meramalkan aliran untuk *steady state* untuk *impellers* dan *baffles* di dalam tangki. *Unsteady solver* digunakan untuk meramalkan penumpahan berkala dan membawa kepada data yang lebih bertepatan dengan data eksperimen yang dicapai menggunakan *steady solver*.

TABLE OF CONTENTS

LIST OF TABLES

LIST OF FIGURES

LIST OF SYMBOLS

σ_k	-	Constant for eq.(3-1)
σ_ε	-	Constant for eq. (3-2)
$C_{1\varepsilon}$	-	Constant for eq. (3-5)
β_{i1}	-	Constant for eq. (3-14)
β_{i2}	-	Constant for eq. (3-14)
$C_{2\varepsilon}$	-	Constant for eq. (3-5)
C_μ	-	Constant for eq. (3-3)
D	-	Impeller diameter, m
ε	-	Turbulent energy dissipation rate
H	-	Liquid height in the tank, m
k	-	Turbulent kinetic energy, $m^2.s^{-1}$
N	-	Rotational speed, s^{-1}
Re	-	Reynolds number
T	-	Tank diameter, m
Utip	-	Impeller tip velocity, $m.^{s-1}$

LIST OF ABBREVIATIONS

SM	-	Sliding mesh
MRF	-	Multiple Reference Frames
CFD	-	Computational Fluid Dynamics
LES	-	Large-eddy Simulation
RANS	-	Reynolds-averaged Navier-Stokes
et al.	-	and others
LDA	-	Laser Doppler Anemometer
PIV	-	Particle Image Velocity
SKE	-	Standard k-ε
RKE	-	Realizable k-ε
SST k-ϖ	-	Shear-stress-transport k-ϖ
HEDT	-	Deep hollow blade (semi-ellipse) disc turbine
RT	-	Rushton turbine

CHAPTER 1

INTRODUCTION

1.1 MOTIVATION

Stirred tank is widely used in chemical, mineral and biochemical industries and waste water treatment. In the majority cases, the flow field in baffled stirred tank is highly turbulent hence it is three-dimensional and complex in nature. There have been continuous efforts on understanding these flows using whether experimental or computational dynamics tools.

Understanding the model and design fluid flow whether single phase or multiple phases would allow for better performance and decrease waste due to inadequate design. More than 15 years ago, it is estimated that nearly half of the $750 billion annual output from chemical industry alone passed through a stirred tank at one point and that losses incurred by inadequate design were on the order of tens of billions of dollars (Tatterson et al., 1991) and about 50% of all chemical productions take place in stirred tank (Butcher and Eagles, 2002). Therefore, adequate design with lower cost can be simulated by using Computational Fluid Dynamics (CFD) to achieved advanced gas dispersion using deep hollow blade turbine.

1.2 PROBLEM STATEMENT

Gas dispersion technology is important. The design must consider the flow filled in baffled stirred tank and turbulent kinetics energy.

For several decades, the Rushton turbine was the standard impeller for gas dispersion applications. It features six flat blades mounted on a disk. The flat blade of the Rushton turbine leads to the formation of a pair of high-speed, low-pressure trailing vortices at the rear of each blade. Those vortices provide the source of turbulence and are identified as the major flow mechanism responsible for mixing and dispersion in stirred tanks. However, the trailing vortices lead to a high power number under ungassed conditions which gives rise to a high torque for a given rotating speed and hence a high operating cost.

Then, John M. Smith and coworkers introduced the concept of using concave blades. They explained the improved performance of the concave blades compared to flat blades in terms of reduced cavity formation behind the blades (Bakker et al., 2000). Hence, the attached gas bubble does not affect the drag in the same way as it does with a flat blade. So the power loss is much less compared with the flat blade. Latterly, impellers with a semi-circular blade shape are introduced for example CD-6 (symmetric blade) and BT-6 (asymmetric blade).

Relatively recent, new blade impeller has been introduced. Deep hollow blade turbine (HEDT) is more effective for gas-liquid dispersion and liquid-liquid dispersion even though it can be used for any type of single-phase and multiple phase mixing duty. As radial flow impellers, it will discharge fluid radially outward to the vessel wall while with suitable baffles these flows are converted to strong top-to-bottom flows above and below the impeller. Therefore, the elliptical shape reduces the cavity size, great reduction of the trailing vortex and results in much less power drop when gassed. HEDT would handle high gas rates without significant loss of power under fully loaded conditions. Therefore, studies on the HEDT are helpful for better gas dispersion in mechanically stirred tank.

Experimental for investigating the structure and behavior of gas dispersion have been done previously using advanced methods such as time-resolved particle image velocimetry (TRPIV) and Laser-Droppler Anemometry (LDA) (Gao et al., 2010). LDA to measure the angle resolved is essentially a single point technique. Therefore, instantaneous measurements of large-scale structures are not possible with LDA. PIV is a whole field technique to characterize instantaneous flow structures around rotating impeller blades. Yet, these methods have limitations according to their affordability as both are expensive, difficulties in set-up and harmful based on the laser used. Thus, computational fluid dynamics (CFD) is an increasingly important tool for carrying out realistic simulations of process equipment (Scargiali et al., 2007). CFD can be used as a design tool or as a design guide to compare the performance of HEDT in stirred tank with decreasing cost to evaluate without undertaking expensive experimental pilot or laboratory to test of all parameters required.

1.3 OBJECTIVE AND SCOPE

The aim of this study is to develop a modeling method for hydrodynamics. In this paper, the flow fields and turbulence kinetics energy in stirred tank with deep hollow blade turbine were investigated by using a computational fluid dynamics (CFD). The CFD model used to validate the flow patterns and gas dispersion performance using HEDT by comparing the results with publish results. The first scope of this research is to predict velocity profile and turbulence kinetics energy (TKE) of stirred tank agitated with HEDT. The second part is to predict the effect of discretisation method and grid analysis.

1.4 SIGNIFICANT OF STUDY

Maximizing profits by operating the most efficient process is the primary goal of all industrial operations such as fermentation, pharmaceutical and biochemical. Process simulation which is the application of a range of software tools to analyze complete processes creates efficient operation at inexpensive workstations. In addition, many qualitative features of the flow field can be difficult to be determined experimentally. Process engineers and scientists use simulation models to investigate complex and integrated biochemical operations without the need for extensive experimentation (Gosling, 2005). A recent development in modeling is the use of Computational Fluid Dynamics (CFD). Model developed in this work via CFD is useful tool to investigate single and multiphase stirred tank operations without the need for extensive experimental setup as prototype and pilot scale testing can be time-consuming and expensive. Therefore, studying the fluid dynamics of advanced gas dispersion using deep hollow blade turbine (HEDT) enable to predict and understand the process flow condition while reducing costs and time-to-market.

1.5 MAIN CONTRIBUTION OF THIS WORK

Deep hollow blade turbine (HEDT) is an effective impeller for gas-liquid dispersion and liquid-liquid dispersion for any type of single-phase or multiple phases mixing. Most of the researchers done in mixing area are limited to experimental method to examine the flow structures developed in stirred vessel such as Laser-Doppler Anemometry (LDA) and Particle Image Velocity (PIV) method. Recent publications have established the potential of computational fluid dynamics (CFD) using Rushton impeller which has been recognized for several decades followed by concave blades and impellers with a semi-circular blade shape for example CD-6 (symmetric blade) and BT-6 (asymmetric blade). Therefore, in this work it is necessary to investigate the ability of HEDT as until now, no research available which evaluate turbulence models or flow distributions for mechanical agitation using HEDT by CFD method as this method has now become a powerful tool for prediction of fluid flows and mixing time in stirred vessels.

1.6 STRUCTURE OF THIS WORK

The structure of the thesis is outlined as follow:

Chapter 2, the literature review provides general description on the flow characteristics provided with a brief discussion from the previous work related to advanced experimental techniques available. The applications and limitation of method also stated.

Chapter 3, the CFD approach presenting the turbulence modeling, velocity characteristics and solution procedures.

Chapter 4, the results for effect of discretisation method, grid dependent analysis, effect of turbulence model and comparison between steady and unsteady simulation were compared with predicted results from experimental data. This chapter validates the experimental published data by Gao et al. (2010) with the CFD model.

Chapter 5, the conclusions of this study and recommendations for future work are given.

CHAPTER 2

LITERATURE REVIEW

2.1 OVERVIEW

This chapter will be covered on the description of deep hollow blade turbine (HEDT) that shows the suitability to achieved better gas dispersion. Experimental and simulation work has been reported in the published literature. Hence, the present work reviews on the computational work on the velocity and turbulent kinetics energy

2.2 INTRODUCTION

An impeller that approximately maintains the ungassed power level when gas is introduced will give more stable operation and minimal scale-up difficulties. Deep hollow blade turbine suitable for advance gas dispersion as it will control the flooding point, loaded condition and hold up. Then, flooding point is the point where the gas bubbles are not driven to the tank wall roughly within the plane of the impeller. Therefore, this impeller can avoid flooding which a condition that more gas is entering than it is effectively able to disperse with radial agitators to achieved complete dispersion whereby the gas bubbles are distributed throughout the vessel and significant gas is circulated back to the impeller.

Although they can be used for any type of single-phase and multiple phase mixing duty, they are most effective for gas-liquid dispersion. Radial flow impeller discharge fluid radially outward to the vessel wall while with suitable baffles, this flow is converted to strong top-to-bottom flows both above and below the impeller. Under fully loaded conditions in which the impeller disperses the gas through the upper part of the vessel, the hollow blade turbine will handle high gas rate without significant loss of power. This is a function of the degree of streamlining as the design of blade ensures it achieves the minimum Froude number (Cooke et al., 2005). Froude number is to correlate power draw in gas-liquid systems where gravity has a significant influence due to the low density of gas bubbles and their strong tendency to rise.

Based on the idea that gas rises, the gas pocket or cavities must be eliminated so as to minimize power drop on the low pressure side and high gas flow rates of the blade. So that, deep hollow blade shape reduces the cavity size and provide better gas dispersion as the gas is being dispersed from inside of the blade, reduces streamlining, much less power drop when gassed and increases net pumping. Therefore, it also improves holding up capacity.

2. 3 APPLICATION OF STIRRED TANK DISPERSION

2.3.1 Bioreactor Fermentation

One common goal in plant cell bioreactor design is to develop a reactor that provides a prolonged, sterile, culture environment with efficient mixing and oxygen transfer without producing excessive foaming and hydrodynamics shear at low cost. Down-pumping mode in viscous *Streptomyces* fermentation gave better oxygen transfer with very little power drops of gassing even at very high impeller flow rates. Therefore, deep hollow blade turbine is expected to be well suited for dispersing gas in bioreactors where a wide range of gas is required (Yang et al., 2007).

2.3.2 Reactive Crystallization

Reactive crystallization presents critical mixing issues because mixing affects both the reaction and crystallization step. Those difficulty with reactive crystallization scale-up due to the need to balance the requirements to achieve a growth-dominated process, choose a mixing system fast enough to micro-mix effectively for the fast reaction and ensure mixing is not too powerful that it will cause crystal fracture. Macro mixing performance for the optimization of the configurations and operating conditions provided with fully turbulent flow. Apart from macro mixing performance, micro mixing performance indicators such as turbulent kinetic energy and local energy dissipation rate are also important in processes, especially for crystallization (Li et al., 2005).

2.4 EXPERIMENTAL METHOD OF STIRRED TANK DISPERSION

There are several technique used to study on the gas dispersion which consists of Laser-Doppler Anemometry (LDA) and Time-Resolved Particle Image Velocimetry (TRPIV) instead of Computational Fluid Dynamics (CFD) method.

2.4.1 Laser-Doppler Anemometry (LDA)

Laser-Doppler Anemometry (LDA) is a technology to measure velocities of gasses at a point in a flow using light beams from a laser especially for small particles in flows. This technique senses true velocity and measures the laser light scattered by particles that pass through a series of interference fringes (a pattern of light and dark surfaces). A laser beam is split into two beams with one propagated out of the anemometer. Scattered light from particles passing through is focused and send the light back into a detector to measure relative to the original laser beam. A beat frequency corresponding to the difference in Doppler shifts from the two scattered beams is obtained since the light scattered from both beams reaches the detector simultaneously. Therefore, the beat frequency is directly proportional to the velocity component perpendicular to the fringe geometry which emerges in the cross section.

2.4.2 Time-Resolved Particle Image Velocimetry (TRPIV)

Time-Resolved Particle Image Velocimetry (TRPIV) consists of a laser with sheet optics, one or two digital cameras and a computer with a timer unit to control the system and storing data. The movement of a group of particles flows can be determined as two consecutive short-duration light pulses produced by a laser scattered from the particles is acquired during both laser pulse by a digital camera and stored for analysis. Displacement of the particles between the laser pulses gives estimation of velocity of the particles. As it able to do time-resolve PIV, several thousand velocity fields per second can be obtained.

2.5 STUDIES ON STIRRED TANK DISPERSION

In previous, experimental and CFD studies have been conducted by many researchers. These studies provide valuable information on hydrodynamics in stirred tank using different type of impellers and turbulent model. Some of the work is summarized in Table 2.1. The majority of the results include data which can be used for the validation of further CFD investigation and the optimum design of the blade impeller in stirred tank. Therefore, the aim of this work is to improve the CFD prediction for HEDT impeller in stirred tank.

Table 2.1 Study of deep hollow blade turbine

Authors	**System investigated**	**Turbulence Model**	**Remarks**
Alcamo et al. (2005)	Rushton impeller, unbaffled vessel *D* = 0.19m, *H* = *T*, *N* = 200rpm, *Re* = 3×10^4	Large eddy simulation (LES)	An excellent agreement between experimental data (PIV) for unbaffled vessel and CFD simulation using LES especially regarding mean tangential velocities. Good agreement was also observed for radial average velocities.
Aubin et al. (2004)	Pitched blade turbine, (simulations are validated using experimental LDV results obtained by the same group of authors)	*k*-*ε* model, RNG model	The CFD simulations have been validated by laser doppler velocimetry (LDV). A first order method underestimate LDV data compared to higher order methods. The type of the turbulence model was limited to the k-ε and RNG models due to convergence difficulties encountered with a Reynolds stress model. Little effect on the mean flow and turbulent kinetic energy were found by using those turbulence models.
Gao et al. (2008)	RT6, CD6, HEDT impellers, *T* = 0.48m, *T*/10, *D* = 0.034m, *H* = 0.25m, electrical input = 3, 6,9 and12kW	no	The study proves that HEDT impeller operates well in a boiling suspension, maintaining suspension at lower specific power input rather than BT6 and CD6 impellers.
Gao et al. (2010)	HEDT impeller, *T* = 0.19m, *D* = 0.4T, *H* = *T*, *N* = 90rmin^{-1}, *Re* = 8847	no	This study compared experimental values of radial velocity, axial velocity, vorticity, the random turbulent kinetic energy and periodic kinetic energy obtained from traditional PIV and TRPIV. The evaluation of the impeller stream was observed clearly from both methods.

Table 2.1 Study of deep hollow blade turbine (Continued)

Authors	**System investigated**	**Turbulence Model**	**Remarks**
Gao et al. (2011)	RT, CD, HEDT and PDT impellers, D = 0.48m	no	PIV technique used to study the trailing vortices and the distribution of turbulent kinetic energy. Disc turbine shape of blade decreases the power input. The phase-averaged turbulent kinetic energy show the turbulent kinetic energy becomes smaller as the blade turns more curved. As the blade turns more curved, the inclination of the impeller stream become smaller and the radial jet becomes weaker.
Hartmann et al. (2004)	Sliding mesh (SM), Rushton turbine, T = 150mm, H = T, N = 2627 rpm	Large eddy simulations (LES), Reynolds-averaged Navier-Stokes (RANS) – shear-stress transport (SST) model	A transient RANS simulation is able to provide an accurate representation of flow field but fails in the prediction of the turbulent kinetic energy compared to the LES model.
Jahoda et al. (2009)	Sliding mesh (SM) method, Multiple Reference Frames (MRF) method, PBT impeller, T = 0.29m, T/10, H=T, N = 300 rpm, Re = 4.66x10^4	Standard k-ε Eulerian-Eulerian approach	CFD simulation of a gas-liquid two-phase flow predicted using RANS technique. The results show a good agreement with experiment based on prediction of liquid homogenization using SM method while MRF method is sufficient mainly for higher volumetric gas flow rate.

Table 2.1 Study of deep hollow blade turbine (Continued)

Authors	System investigated	Turbulence Model	Remarks
Jaworski and Zakrzewska (2002)	Pitched blade turbine, T = 0.202m, H = T, N = 290 rpm, Re = 22,500	Standard k-ε, RNG k-ε model, realizable k-ε model, Chen-Kim k-ε, optimized Chen-Kim k-ε, Reynolds stress model	Simulation results were compared with LDA experimental data. The axial velocity component was predicted well by using standard k-ε model and the optimized Chen-Kim k-ε model while turbulent kinetic energy was significantly underpredicted for all models. However, standard k-ε delivered the smallest deviations from experiment.
Khopkar et al. (2006)	Pitched blade turbine, T = 0.3m, H = 0.9m, T/10, N = 100, 145 and 390 rpm, d_s = 0.1mm	Standard k-ε	CFD model used to investigate the turbulent gas-liquid flows generated by three down-pumping pitched blade turbines. Flow field generated by three-down pumping pitched blade turbine, including the liquid circulation loops and the dispersion quality of gas is captured.
Kshatriya et al. (2007)	Multiple Reference Frame (MRF) method, BT6, ICI gasfoil, PBIUP and PBIDIN impeller, N = 10rps, superficial gas flow = 0.130 m/s, D = 0.57m,	k-ω model	CFD is shown as a useful tool to predict the experiment on cavity formation on impeller and gas dispersion pattern (gas holdup and transition regimes). Larger the cavity, larger the power drop. Based on experimental observation and CFD performance, PBIUP gives a better gas performance. PBIUP is modified impeller which made asymmetric with the extension of upper part.

Table 2.1 Study of deep hollow blade turbine (Continued)

Authors	System investigated	Turbulence Model	Remarks
Murthy and Joshi (2008)	DT, PBT (60,45 and 30) and HF impeller, $H = T$, $T/10$, $T = 0.30$m,	Standard k-ϵ Reynolds stress model (RSM) Large eddy simulation (LES)	Mean flow field and turbulent kinetic energy measured using LDA was compared with CFD simulations performed by Standard k-ϵ, Reynolds stress model (RSM) and Large eddy simulation (LES). For mean flow predictions, RSM performed better than the standard k-ϵ as standard k-ϵ performs well when the flow is unidirectional that is with less swirl and weak recirculation. Both Standard k-ϵ and RSM fail to predict the turbulent kinetics energy in the impeller region when the flow is dominated by the unsteady coherent flow structures. However, LES has strength of the precessing vortex instability and turbulent kinetics energy. So DT has identified produces strongest instabilities while HF generates the weakest instabilities.
Myer et al. (1999)	BT-6, PD-6, D-6 and CD-6 impellers, $D = 0.44$m, 0.60m and 1.52m, $T/12$, superficial gas velocity = 0.007-0.07ms^{-1}, power input = 400-4000Wm^{-3}, Re = 10-2000000	no	From experiment data, performance of gas dispersion can be significantly improved by using deep blades that are vertically asymmetric. It has a gassed number which lower than other impellers. It also can disperse more gas before flooding and no gas filled cavities were observed from the inside of the blade.

Table 2.1 Study of deep hollow blade turbine (Continued)

Authors	System investigated	Turbulence Model	Remarks
Scargiali et al. (2007)	Sliding mesh (SM) model, T = 0.45m, T/12, N = 376rpm, d_s = 3mm	Standard k-ε Eulerian-Eulerian multi-fluid approach	CFD simulation of gas-liquid dispersion in acceptable agreement with experiment. Gas-liquid stirred vessels are essentially dominated by drag, buoyancy and convection.
Smith et al. (2001)	D-6,CD-6,BT-6 and ICI Quasi GF impellers,	no	This study demonstrated that there are significant differences between hot sparged and cold sparged conditions in power draw and flooding behaviour.
Wu (2011)	Sliding mesh (SM) model, Multiple Reference Frame (MRF) model, Lightnin A310 and PMSL 3LS30 impeller, T = 12m	Standard k-ε,RNG k-ε model, realizable k-ε model, standard k-ω model, SST k-ω model and Reynolds stress model	The model validation is conducted by comparing the simulated velocities with experimental data. The realizable k-ε model and standard k-ω model are found to be more appropriate than other turbulence models.
Wang and Mao (2006)	Rushton impeller, T = 0.45m, T/10, d_s = 76mm	Standard k-ε Eulerian-Eulerian approach	Comparison between CFD and experimental data on the gas-liquid flow pattern transition as the stirring speed or rate of aeration is changed shows acceptable agreement. Gas holdup nonuniformly and decrease with the radial position are also clearly reflected by the simulation.
Zadghaffari et al. (2010)	Sliding mesh, Rushton turbine, T = 270mm, 0.1T, H = T,N = 200rpm	Large eddy simulation (LES)	The predicted time averaged radial, axial and circumferential velocities were using CFD simulation shown good agreement with experimental data (LDA). Comparison of LES and RANS predictions of the tracer concentration profile with experimental data indicated that improved predictions can be achieved with LES than RANS.

2.6 SUMMARY

Stirred vessels have wide applications in the chemical industries such as bioreactor fermentation and reactive crystallization. The experimental and simulation work has been outlined in this chapter. From the description above, there are reviews on experimental work on the velocity and turbulent kinetics energy by HEDT impeller (Gao et al., 2010 and Gao et al., 2011) using traditional PIV method. The HEDT impeller is recommended for usage which resulted in better gas dispersion at lower specific power input rather than BT6 and CD6 impellers (Gao et al., 2008). It has gassed number which lower than other impellers and no gas filled cavities were observed from the inside of the blade (Myer et al., 1999).

Four commonly used turbulence model for stirred tank simulation were standard k-ε, realizable k-ε, shear-stress transport k-ϖ and large-eddy simulation (LES). Standard k-ε model is the most widely used turbulence model as the robustness, economy and reasonable accuracy compared to other models. From research of Jaworski and Zakrzewska (2002), simulation results were compared with LDA experimental data. The axial velocity component was predicted well by using standard k-ε model and the optimized Chen-Kim k-ε model while turbulent kinetic energy was significantly underpredicted for all models. Standard k-ε delivered the smallest deviations from experiment as this model suitable for usage of high Reynolds number (22,500). Jahoda et al. (2009) investigated mixing of PBT impeller in 0.29 m diameter tank. From their studies, standard k-ε solved with multiple reference frame (MRF) method sufficiently for higher volumetric gas flow rate while sliding mesh (SM) method shows a good agreement with experimental data. However, the standard k-ε model has deficiencies such as poorly simulating non-equilibrium boundary layers. Therefore, there is intense research of the other turbulence model to improve it including examine on realizable k-ε model.

Realizable k-ε model and standard k-ϖ model are highly recommended to predict mechanical agitation of non-Newtonian fluids at six TS levels (Wu, 2011). The study included comparison between six turbulence models (standard k-ε, RNG k-ε, realizable k-ε, standard k-ϖ, SST k-ϖ and Reynolds stress model). This is based on the turbulence model analysis have proved that Realizable k-ε model and standard k-ϖ model were more appropriate than other turbulence models.

Kshatriya et al. (2007) assessed the shear-stress transport k-ϖ model for comparison between BT6, ICI gas foil, PBIUP and PBIDIN impeller. Then, the CFD predictions were compared with the experimental data. Based on experimental observation and CFD performance, PBIUP which made of modified the extension upper part into asymmetric blade gives a better performance in terms of high relative power draw and prediction of gas holdup.

A promising alternative is large-eddy simulation (LES). LES has strength of the processing vortex instability, turbulent kinetics energy (Murthy and Joshi, 2008) and radial average velocities (Alcamo et al., 2005). LES and RANS simulations were assessed by means of detailed LDA experiments globally throughout the tank and locally near the impeller by Hartmann et al. (2004). The turbulence model used is shear-stress transport (SST). A transient RANS simulation is able to provide an accurate representation of the flow field, but fails in prediction of the turbulent kinetic energy in the impeller region and discharge flow where most of the mixing takes place compared to the LES simulation. However, LES is time consuming and a high-performance computing model especially for industrial applications. Therefore, test on the accuracy of recently available turbulence models that are computationally less demanding than LES are more practical to be investigated.

CHAPTER 3

CFD APPROACHES

3.1 OVERVIEW

Computational Fluid Dynamics (CFD) is a recent used process simulation modeling which is the application of software tool to help create efficient operations by analyzing complete processes. Commercial software packages, FLUENT can model the mixing effect by incorporating physical properties of fluids and aeration patterns, together with the detailed information of vessel internals, such as impeller geometry and baffle location (Gosling, 2005). First, CFD programs used to identify velocity profiles within the fluid to model gas dispersion and turbulent kinetics energy. Then, the result such as areas of poor mixing or areas of high fluid shear can be obtained. Validation of the result was performed using those studied by Gao et al. (2010). Once validated, the same model used to examine single phase mixing hydrodynamics by using Multiple References Frames (MRF) and effect of turbulence model has been carried out for only the case of HEDT using grid resolutions of standard k-ε, realizable k-ε and SST k-ω. The discretisation method and comparison between steady and unsteady simulation also can be investigated.

3.2 INTRODUCTION

Gas dispersion application can be seen from fermentation, pharmaceutical and bioprocessing industry. It is a future technology as investigation of the gas dispersion characteristics of the impeller leading to need of power consumption and oxygen transfer in order to establish a reliable criterion for the predictive scale-up of fermentation results. There are several experimental methods such as Laser-Doppler Anemometry (LDA) and Time-Resolved Particle Image Velocimetry **(**TRPIV) to evaluate the flow patterns on mixing process. Both of these methods are expensive to be established and harmful as the usage of powerful laser in their measurement of turbulent flows. Therefore, CFD model shows promising results and seems to be able to predict gas-liquid flow at any flow regime (Khopkar et al., 2006). Turbulence flow which gives high accuracy in gas dispersion calculation well predicted by CFD.

One advantages with CFD based prediction methods is that they do not have scaling up or scaling down problems as they solve the fundamental equations governing fluid flow. So, some approximation on the physical phenomena, such as phenomenological models for turbulence, is often required, even in the CFD simulations (Zadghaffari et al., 2010). Researchers have employed mainly Reynolds Averaged Navier-Stokes (RANS) techniques to close the equations involved with Reynolds stresses (Yeoh et al., 2004). The result of this kind of method is to achieve good agreement with the experimental measurements in terms of bulk mean flow in the agitated tank, but they suffer from inaccurate turbulent kinetic energy distribution prediction, especially in the region close to the impeller due to the isotropic nature of the k-e turbulence model (Mostek et al., 2005). Large-eddy simulation (LES) first adopted in a stirred tank have proved to be good method of investigating unsteady behavior in turbulent flow (Eggels et al., 1996). LES could provide details of the flow field that cannot be obtained with RANS and corresponding models (Revstedt et al., 1998). However, it is still too computationally expensive to run on a personal computer.

In CFD, fully predictive simulations of the flow field and mixing time mainly use either the sliding mesh (SM) (Murthy et al., 1994) or the multiple reference frame (MRF) (Luo et al., 1994) approaches for account impeller revolution. The SM approach is a fully transient approach, where the rotation of the impeller is explicitly taken into account while the MRF approach predicts relative to the baffles. The SM approach is more accurate but it also much more time consuming than the MRF approach. SM simulation of a stirred tank content homogenization was first published by using the standard k-e model and compared the results with the experimental data (Jaworski and Dudczak, 1998).

SM simulates the interaction between the impellers and the baffles using a CFD package. For estimation of the trends of the homogenization curves, the MRF technique is sufficient mainly for higher volumetric gas flow rate. The main advantage of this method is relatively low computational time with acceptable results (Jahoda et al., 2009). The computational model qualitatively captured the overall flow field generated including the liquid circulation loops and the dispersion quality of gas in reactor. It was also found to simulate the variation in the power dissipation by impellers in the presence of gas and the total gas hold-up reasonably well. The computational model was then used to study the circulation time distribution. The prediction circulation time distribution was found to capture the influence of prevailing flow regimes on the mixing process (Khopkar et al., 2006). Therefore, CFD techniques are increasingly used as a substitute for experiments to obtain detailed flow field for a given set of fluid, impeller and tank geometries (Ranade et al., 1991).

3.3 TURBULENCE MODELLING

Experimental analysis of HEDT has been studied by researchers in the past. Most of the researches focus on the velocity profile, turbulence structure and trailing vortices. Prediction of fluid mixing is important in many chemical process applications. Swirl action imposed on the fluid outflow from HEDT impeller lead to turbulence flow. In turbulent flows, large-scale eddies with coherent structures are mainly responsible for the mixing.

The selection of a turbulence model is very important. Large Eddies Simulation (LES) turbulent model has potential in understanding the fluid flow behaviors. Large eddies are resolve directly and small eddies are modeled. Consequently, modeling using the Reynolds-averaged Navier-Stokes (RANS) turbulence models gives poor prediction. The LES approach is more general than the RANS approach, and avoids the RANS dependence on boundary condition for the large scale eddies. As computational resources are expensive in practical applications of LES, the predictive capabilities of standard k-ε (SKE), realizable k-ε (RKE) and shear-stress-transport k-ω have been extensively compared in this work. These are describing in more detail below.

3.3.1 Standard *k-ε*

The standard k-ε model has become workhorse of practical engineering flow calculations in the time since it was proposed by Launder and Spalding, 1974. Robustness, economy and reasonable accuracy for a wide range of turbulent flows explain its popularity in industrial flow simulations. It is a semi-empirical model based on model transport equations for the turbulence kinetic energy (k) and its dissipation rate (ε). In the derivation of the k-ε model, the assumption is that the flow is fully turbulent, and the effects of molecular viscosity are negligible. Therefore, the standard k-ε model is only valid for fully turbulent flows.

The turbulence kinetic energy, k and its dissipation rate, ε are obtained from the following transport equation:

$$\underbrace{\frac{\partial(\rho k)}{\partial t}}_{time\ derivative} + \underbrace{\frac{\partial}{\partial x_i}(\rho \mu_i k)}_{convection} = \underbrace{\frac{\partial}{\partial x_i}\left(\left(\mu + \frac{\mu_t}{\sigma_k}\right)\frac{\partial k}{\partial x_i}\right)}_{diffusion} + \underbrace{\rho P_k}_{production} - \underbrace{\rho \varepsilon}_{destruction} \qquad Eq\ (3-1)$$

And,

$$\underbrace{\frac{\partial(\rho \varepsilon)}{\partial t}}_{time\ derivatives} + \underbrace{\frac{\partial}{\partial x_i}(\rho \mu_i \varepsilon)}_{convection} = \underbrace{\frac{\partial}{\partial x_i}\left(\left(\mu + \frac{\mu_t}{\sigma_\varepsilon}\right)\frac{\partial \varepsilon}{\partial x_i}\right)}_{diffusion} + \underbrace{S\varepsilon}_{source\ term} \qquad Eq(3-2)$$

The turbulent (eddy) viscosity, μ_t is obtained from:

$$\mu_t = \rho C_\mu \frac{k^2}{\varepsilon} \qquad Eq\ (3-3)$$

The relation for the production term, P_k for the k-ε variant model is given as:

$$P_k = \mu_t \left(\frac{\partial u_j}{\partial x_i} + \frac{\partial u_i}{\partial x_j}\right)\frac{\partial u_j}{\partial x_i} \qquad Eq(3-4)$$

For standard k-ε model the source term, $S\varepsilon$ is given by:

$$S\varepsilon = \rho(C_{1\varepsilon}\frac{\varepsilon}{k}P_k - C_{2\varepsilon}\frac{\varepsilon^2}{k} \qquad Eq(3-5)$$

The model constant are (Launder and Spalding, 1974):$\sigma_k = 1$, $C_{1\varepsilon} = 1.44$,

$C_{2\varepsilon} = 1.92$, $\sigma_\varepsilon = 1.3$, $C_\mu = 0.09$, derived from correlations of experimental data.

3.3.2 Realizable *k-ε*

As the strengths and weaknesses of the standard *k-ε* model have become known, improvement has been made to the model through realizable *k-ε* model. It is more accurately predicts flow features such as strong streamline curvature, vortices and rotation. The realizable *k-ε* model is relatively differs from the standard *k-ε* model in two ways. Firstly, it has new formulation of the turbulent viscosity and secondly, it employs a new transport equation for the dissipation rate. Realizable *k-ε* model still has a similar equation for μ_t as *k-ε*, but C_μ is no longer a constant and instead is a function of velocity gradients given as:

$$C_\mu = \frac{1}{A_o + A_s \frac{U^* k}{\varepsilon}} \qquad Eq\ (3-6)$$

With $A_o = 4.04$, $A_s = \sqrt{6} cos\phi$, $\phi = \frac{cos^{-1}(\sqrt{6}w}{3}$, $w = \frac{S_{ij}S_{jk}S_{ki}}{\tilde{S}^3}$,

$U^* = \sqrt{S_{ij}S_{ij} + \tilde{\Omega}_{ij}\tilde{\Omega}_{ij}}$ and $\tilde{S} = \sqrt{S_{ij}S_{ij}}$ to ensure positivity of normal stresses ($\overline{u_i^2} \geq 0$) and Schwarz's inequility for shear stress $\left(\left(\overline{u_i u_j}\right)^2 \leq \overline{u_i^2}\,\overline{u_j^2}\right)$. The Schwarz inequality for shear stresses in k-e model can be violated when the mean strain rate is large, but it can be eliminated by having a variable C_μ (Fluent 6.2, 2005)

The source term, $S\varepsilon$ for realizable *k-ε* model is now given as:

$$S_\varepsilon = \rho(C_1 S_\varepsilon - C_2 \frac{\varepsilon^2}{k + \sqrt{v\varepsilon}} \qquad Eq\ (3-7)$$

This model constants are (Shih et al., 1995): $\sigma_k = 1.0$, $\sigma_\varepsilon = 1.2$, $C_2 = 1.9$, $C_1 = \max[\ 0.43, \frac{\eta}{\eta+5}]$, with $\eta = S\frac{k}{\varepsilon}$ and $S = \sqrt{2S_{ij}S_{ij}}$ is a modulus of mean rate of strain tensor.

3.3.3 Shear-stress transport *k-ω*

The shear-stress transport *k-ω* model was developed to effectively blend the robust and accurate formulation of the *k-ω* model in the near wall-region with the free-stream independence of the *k-ω* model in the far field. In order to achieve this, the *k-ε* model is converted into a *k-ω* formulation. The turbulence kinetic energy, k and its dissipation rate, ω are obtained from the following transport equation:

$$\underbrace{\frac{\partial(\rho k)}{\partial t}}_{time\ derivative} + \underbrace{\frac{\partial}{\partial x_i}(\rho \mu_i k)}_{convection} =$$

$$\underbrace{\frac{\partial}{\partial x_i}\left(\left(\mu + \frac{\mu_t}{\sigma_k}\right)\frac{\partial k}{\partial x_i}\right)}_{diffusion} + \underbrace{\bar{G}_k}_{production} - \underbrace{Y_k}_{dissipation} + \underbrace{S_k}_{dsource\ term} \qquad Eq\ (3-8)$$

And

$$\underbrace{\frac{\partial(\rho \omega)}{\partial t}}_{time\ derivatives} + \underbrace{\frac{\partial}{\partial x_i}(\rho \mu_i \omega)}_{convection} =$$

$$\underbrace{\frac{\partial}{\partial x_i}\left(\left(\mu + \frac{\mu_t}{\sigma_\omega}\right)\frac{\partial \omega}{\partial x_i}\right)}_{diffusion} + \underbrace{G_\omega}_{production} - \underbrace{Y_\omega}_{dissipation} + \underbrace{D_\omega}_{cross-diffusion}$$

$$+ \underbrace{S\omega}_{source\ term} \qquad Eq(3-9)$$

The turbulent viscosity, μ_t is computed from:

$$\mu_t = \frac{\rho k}{\omega} \frac{1}{\max\left[\frac{1}{\alpha^*}, \frac{SF_2}{\alpha_{1\omega}}\right]} \qquad Eq\ (3-10)$$

The term $\bar{G}_k$ represents the production of turbulence kinetic energy, and is defined as:

$$\bar{G}_k = \min(G_k, 10\rho\beta^* k\varpi) \qquad Eq(3-11)$$

Where G_k is defined as $G_k = \mu_t S^2$ (in a manner consistent with the Boussinesq hypothesis). S is the modulus of the mean rate-of-strain tensor, $S = \sqrt{2S_{ij}S_{ij}}$.

The term G_ϖ represents the production of ϖ and is given by:

$$G_\varpi = \frac{\alpha}{v_t}\bar{G}_k \qquad Eq(3-12)$$

The term Y_k represents the dissipation of *k*, and is defined

$$Y_k = \rho\beta^*\varpi^2 \qquad Eq(3-13)$$

While the term Y_ϖ represents the dissipation of ϖ, and is defined

$$Y_\varpi = \rho\beta\varpi^2 \qquad Eq(3-14)$$

Where $\beta_i = F_1\beta_{i1} + (1-F_1)\beta_{i2}$ and $F_1 = \tanh(\phi_1^4)$

This model is based on both the standard *k*-ϖ model and *k*-ε model. To blend these two models together, the standard *k*-ε model has been transformed into equation based on *k* and ϖ, which leads to the introduction of a cross-diffusion term, D_ϖ :

$$D_\varpi = 2(1-F_1)\rho\sigma_{\varpi 1}\frac{1}{\varpi}\frac{\partial k}{\partial x_j}\frac{\partial \varpi}{\partial x_j} \qquad Eq(3-15)$$

For standard k-ε model the source term, $S\varepsilon$ is given by:

$$S\varepsilon = \rho(C_{1\varepsilon}\frac{\varepsilon}{k}P_k - C_{2\varepsilon}\frac{\varepsilon^2}{k} \qquad Eq(3-5)$$

The model constant are (Menter, 1994):$\sigma_{k1} = 1.176$, $\alpha_{\varpi 2} = 1.168$, $\alpha_{\varpi 1} = 2.0$, $\sigma_{k2} = 1.0$, $\alpha_1 = 0.31$, $\beta_{i1} = 0.075$, $\beta_{i2} = 0.0828$.

3.4 NUMERICAL DETAILS

3.4.1 Geometrical details and grid generation

The CFD model was validated with experimental results from Gao et al. (2010) as shown in Figure 3.1. The Reynolds number was 8847; impeller rotational speed was 90 $r.min^{-1}$ and fitted with four baffles of width T/10 was used as stirred vessel for analysis of turbulence structure in the stirred tank with a deep hollow blade disc turbine by time-resolved PIV. GAMBIT mesh generated tool used for meshing the hexahedral geometry and ensure a good quality of mesh. Therefore, impeller blades and baffles were considered zero thickness in order to ensure better quality of mesh.

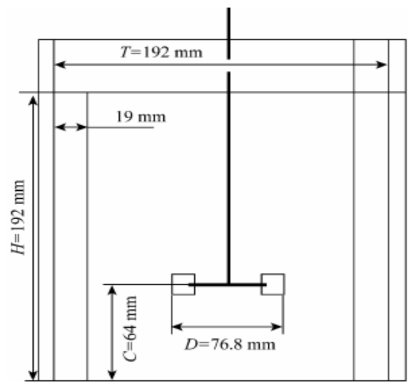

Figure 3.1: The geometry of the experimental tank

3.5 METHOD OF SOLUTION

The computational work has been carried out using the commercially software FLUENT 6.3 to stimulate the parameters chosen. FLUENT's moving reference frame modeling capability allows to model problems involving moving parts by allowing activating moving reference frames in selected cell zones. In most cases, the moving parts render the problem unsteady when viewed from the stationary frame. However, the flow around the moving part can (with certain restrictions) be modeled as a steady-state problem with respect to the moving frame (Fluent 6.3, 2006). The PRESTO scheme is well suited for steep pressure gradients involved in rotating flows. It provides improved pressure interpolation in situations where large body forces or strong pressure variations are present as in swirling flows.

In order to ensure smooth and better convergence initially k-ε simulations have been performed until the complete steady flow is obtained. Then, effect of turbulence model has been carried out for only the case of HEDT using grid resolutions of standard k-ε, realizable k-ε and SST k-ϖ. The total number of cells in the five directions for the cases (807k, 1016k, 1066k, 1100k and 1333k) has been found that all the grids gave very similar profiles of turbulence kinetic energy, axial and radial velocity towards experimental results. Effect of discretisation and comparison between steady solver and unsteady solver has also been identified through simulation.

CHAPTER 4

RESULTS AND DISCUSSIONS

4.1 INTRODUCTION

CFD simulations were performed using three different turbulent model, standard *k*-*ε* (SKE), realizable *k*-*ε* (RKE) and Shear-stress-transport *k*-*ϖ* (SSTKW). The study includes influence of discretisation method, grid dependent analysis, effect of turbulence model and comparison between steady and unsteady flow. All the simulation prediction has been compared with experimental data from Gao et al. (2010).

4.1.1 Influence of Discretisation Method

The first order upwind scheme is the default setting in Fluent. This is the simplest scheme which used earlier in the discretisation to start off a calculation. The value at the face is assumed the same as the cell centered value in the cell upstream of the face. The main advantages of first order upwind scheme is easy to implement which resulting in very stable calculations. If the flow is aligned with the grid, first-order scheme are acceptable. However, this scheme overestimates the transport in flow direction, hence gives rise to numerical diffusion. Therefore, a switch to a higher-order scheme is usually recommended once the solution has partially converged as computing time can be saved.

The second order upwind scheme may be applied to improve the simulation accuracy (Fluent, 2005). The improvement is based on the fact that two upwind nodes are taken into account when estimating the upwind face value. It is assumed that the gradient between the present node and the eastern face is the same as between downwind node and the present node.

Two different discretisation namely the first order and second order scheme was used together with the steady standard *k-ε* model to evaluate the effect of the discretisation scheme. Simulations were performed using the intermediate grid and compared with experiment studied by Gao et al. (2010) in Figure 4.1.

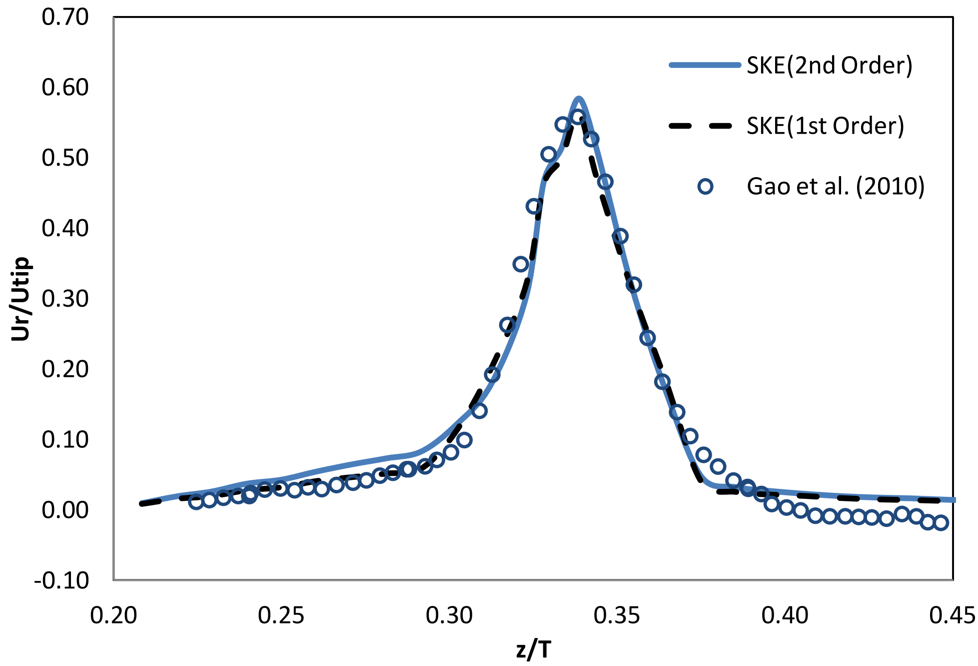

(a) Radial Velocity

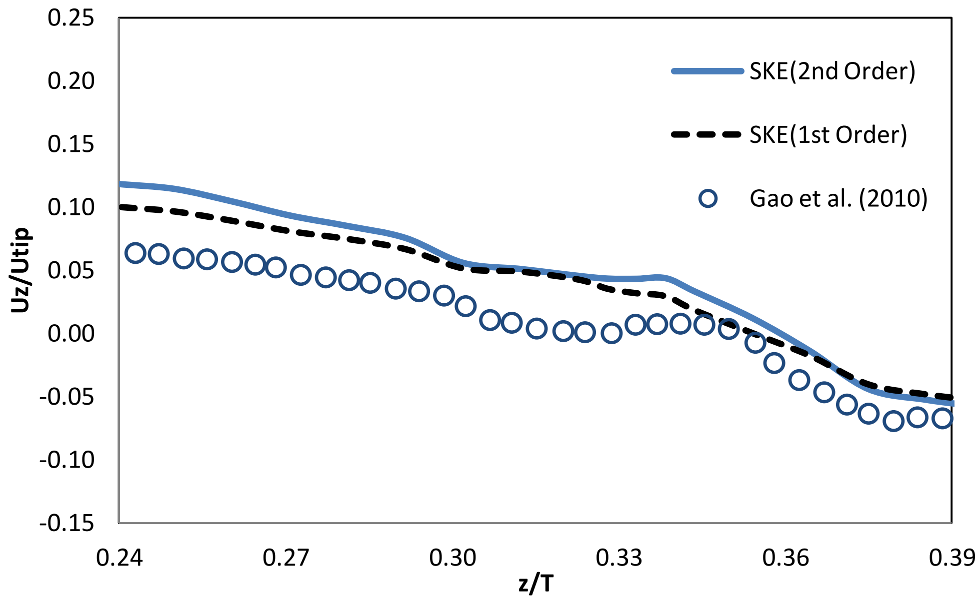

(b) Axial Velocity

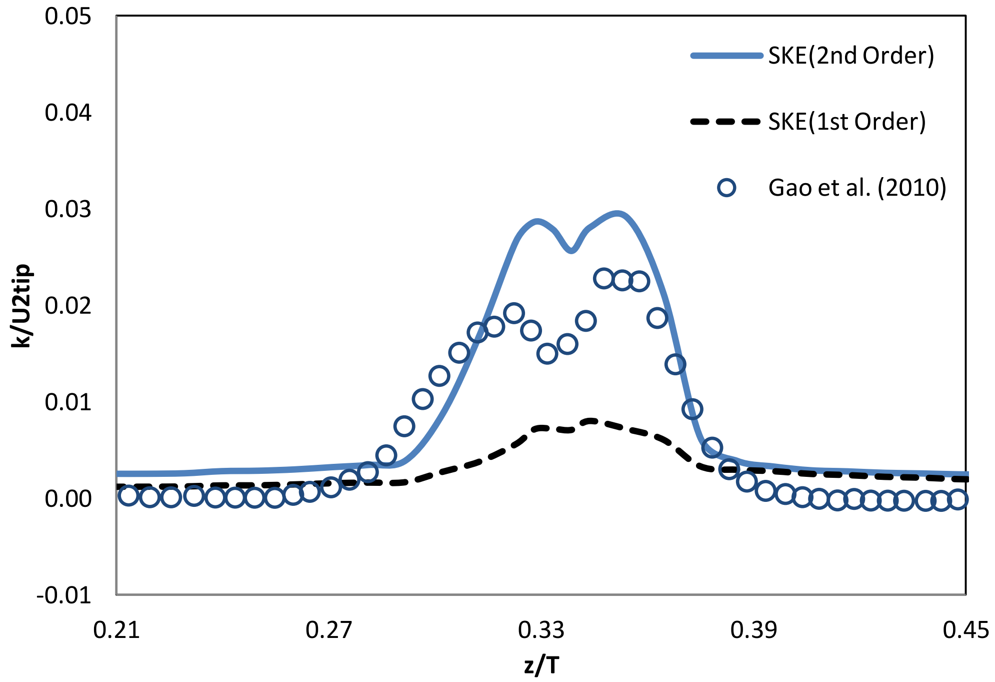

(c) Axial distribution of random turbulent kinetic energy

Figure 4.1 Influence of Discretization Method at r/T=0.245 of (a) Radial Velocity (b) Axial Velocity (c) Axial distribution of random turbulent kinetic energy

Two types of discretisation namely the first order and second order scheme was used to evaluate the effect of the discretisation scheme for radial velocity profiles, axial velocity profiles and turbulent kinetic energy. The discretisation method is an important observation as it suggests that the prediction of turbulent kinetic energy is dependent not only on the choice of turbulence model as previously suggested by other authors but also on the differencing scheme as the first order scheme does not always to be less accurate in all cases. Aubin et al. (2004) used the first order scheme as from his results, it appears that the first order upwind scheme predicts lower values of turbulent kinetic energy than the higher order one schemes and more closely to the experimental data. Observation from figure 4.1 shows the predictions using the first order and second order scheme is essentially identical with experimental data for radial and axial velocity. But, there are large differences between first order and second order scheme for random turbulent kinetic energy. Therefore, the first order discretisation scheme is significantly less accurate in this work as it leads to more severe underestimation of the kinetic energy and unable to resolve the two peaks exist in the impeller stream. So, the second order scheme was applied to all simulations described hereafter due to reduce the numerical errors in the final solution.

4.1.2 Grid Dependent Analysis

It is necessary to carry out grid dependent analysis for CFD simulation to ensure the result was obtained was accurate and not affected by grid density. The different grids (coarse: 1333k cells and 1100k cells, intermediate: 1066k cells, very coarse: 1016k cells and 807k cells) were shown as Table 4.1. In order to assess the suitability of mesh in this work, combination of hexahedral and tetrahedral element used. Standard k-ε model with steady state solver was employ in this study to evaluate the five different grids. The results from these five different grid densities also compared with the experimental data from Gao et al. (2010).

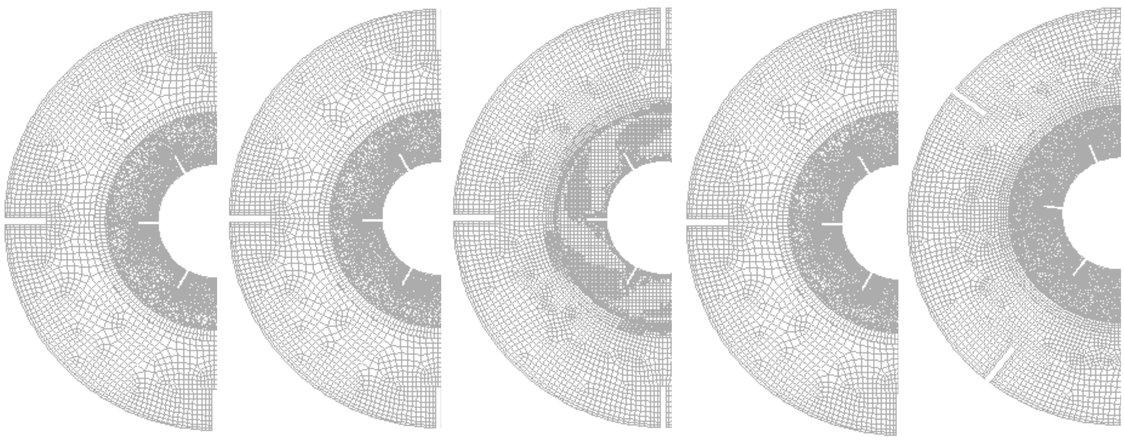

Grid1 ≈	**Grid 2** ≈	**Grid 3** ≈	**Grid 4** ≈	**Grid 5** ≈
807k cells	1016k cells	1066k cells	1100k cells	1333k cells

Table 4.1 Grid display at z = 0.064m

The result from grid dependent study is shown in Figure 4.2.

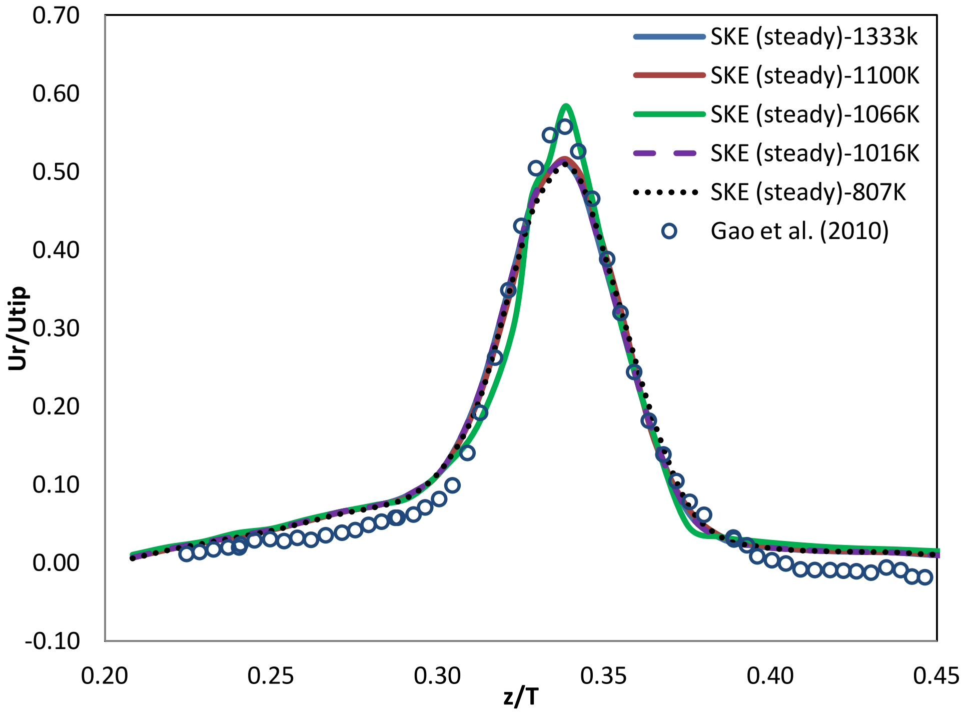

(a) Radial Velocity

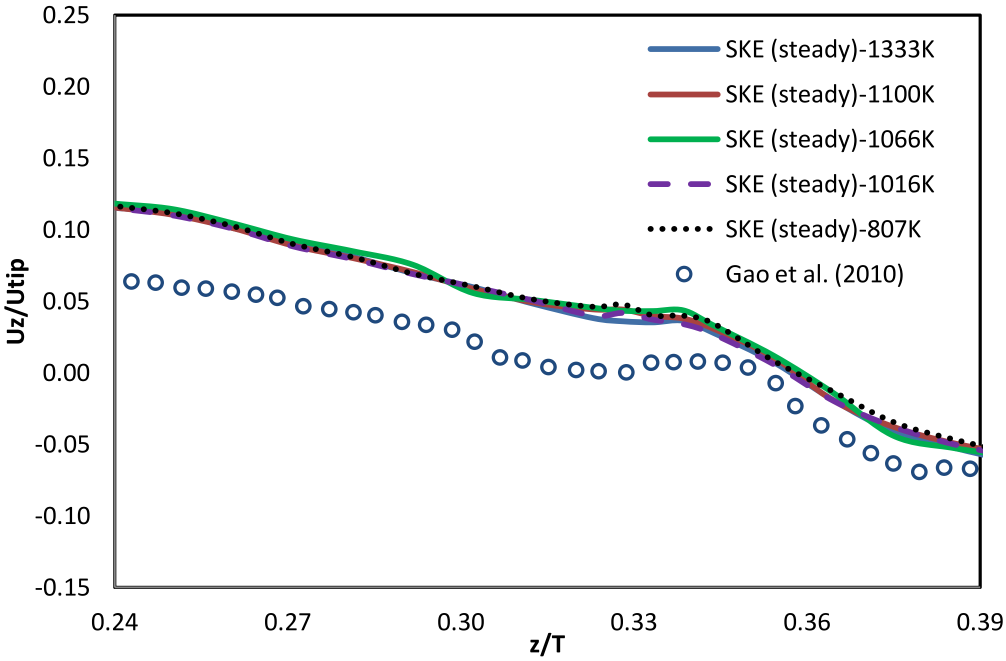

(b) Axial Velocity

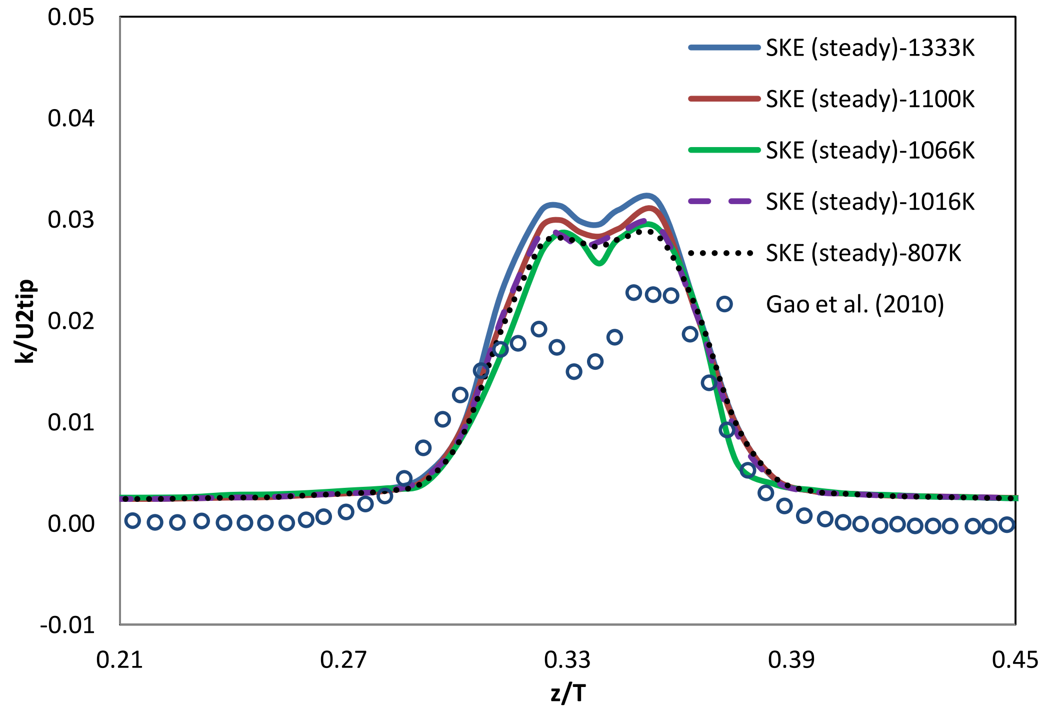

(c) Axial distributions of random turbulent kinetic energy

Figure 4.2 Comparison grid dependent with experiment measurement at r/T= 0.245 of (a) Radial Velocity (b) Axial Velocity (c) Axial distributions of random turbulent kinetic energy

A preliminary grid convergence study was carried out in order to verify that the solution is grid dependent or independent. Because of the Reynolds number investigated in the present work is at lower limit of turbulent regime (Re = 8847), the performance of the sub grid-scale models applied in should be checked (Hartmann et al., 2004). As a fine-grid resolution was used, the results might nearly resemble the results.

There are generally minimal differences between coarse mesh (1333k and 1100k) and very coarse mesh (807k and 1016k) for comparison of radial and axial velocity. The predicted radial and axial velocity profiles agree satisfactorily with the experimental data. Conversely, the magnitudes of the random turbulent kinetic energy were slightly over-predicted even though the trends and the locations of its maximum values were predicted well with the experiment data. Improvement on prediction accuracy can be observed when the mesh density at 1066k for radial, axial and random turbulent kinetic energy. Therefore, the 1066k grid was used for the remaining of this work as it is selective adaptive region than other grids.

4.1.3 Effect of turbulence model

Three different turbulent model used in this work were standard *k-ε* (SKE), realizable *k-ε* (RKE) and shear-stress-transport *k-ϖ* (SSTKW).

The standard *k-ε* model is essentially a high Reynolds number model and assumes the existence of isotropic turbulence and the spectral equilibrium. In the k-*ε* model, the length and the time scales are built up from the turbulent kinetic energy and the dissipation rate using the dimensional arguments. The *k-ε* turbulence models suffer from the necessity of modeling a number of quantities for which reliable experimental data are desirable under a large number of flow conditions. While this necessity is a fundamental weakness of the *k-ε* approach, a further uncertainty lies in the assumption that the turbulent kinetic energy and its dissipation rate are necessary and sufficient turbulence variable for the simulation of turbulent flows. Nonetheless, the model is widely used and has been attributed to some significant simulation successes (Murthy and Joshi, 2008).

Improvements have been made to improve standard *k-ε* capability through introduction of realizable *k-ε* model. One of the more successful recent developments is the realizable *k-ε* model developed by Shih et al. (1995). It contains a new transport equation for the turbulent dissipation rate, ε and a critical coefficient of the model, is expressed as a function of mean flow and turbulence properties instead of assuming it to be constant as in the standard model. Therefore, this allows the model to satisfy certain mathematical constraints on the normal stresses consistent with the physics of turbulence (realizability). A substantial improvement over the standard *k-ε* model as it considers flow curvature features such as strong streamline curvature, vortices and rotation. This model also works well for most flows in baffled vessels. However, due to the fact that the realizable *k-ε* model includes the effects of mean rotation in the definition of the turbulent viscosity, it produces non-physical turbulent viscosities when the computational domain contains both rotating and stationary fluid zones. Since initial studies have shown that the realizable *k-ε* model provides the best performance of all the *k-ε* model versions for several validations of separated flows and flows with complex secondary flow features, realizable *k-ε* had shown a better choice of turbulence model (Fluent, 2009).

The shear-stress-transport *k-ϖ* model is an eddy-viscosity model which includes two main novelties. Firstly, it is combination of a *k-ϖ* model (in the inner boundary layer) and *k-ε* model (in the outer region of and outside of the boundary layer). The *k-ϖ* model is better at predicting adverse pressure gradient but it is dependent on the free-stream value of ϖ. Therefore, combining the two models, *k-ϖ* model and *k-ε* model could improve both of these models. Secondly, a limitation of the shear stress in adverse pressure gradient regions is introduced. Refinements of this model includes blending function which designed to be one in the near-wall region, which activates the standard k-ϖ model and zero away from the surface, which activates the standard *k-ε* model. This model incorporates a damped cross-diffusion derivative term in the ϖ equation. These features make the shear-stress-transport *k-ϖ* model more accurate and reliable for a wider class of flows than the standard *k-ε* model.

The effect of turbulence model on using the standard *k-ε* model, realizable *k-ε* model and shear-stress-transport *k-ϖ* model were compared with experiment studied by Gao et al. (2010).

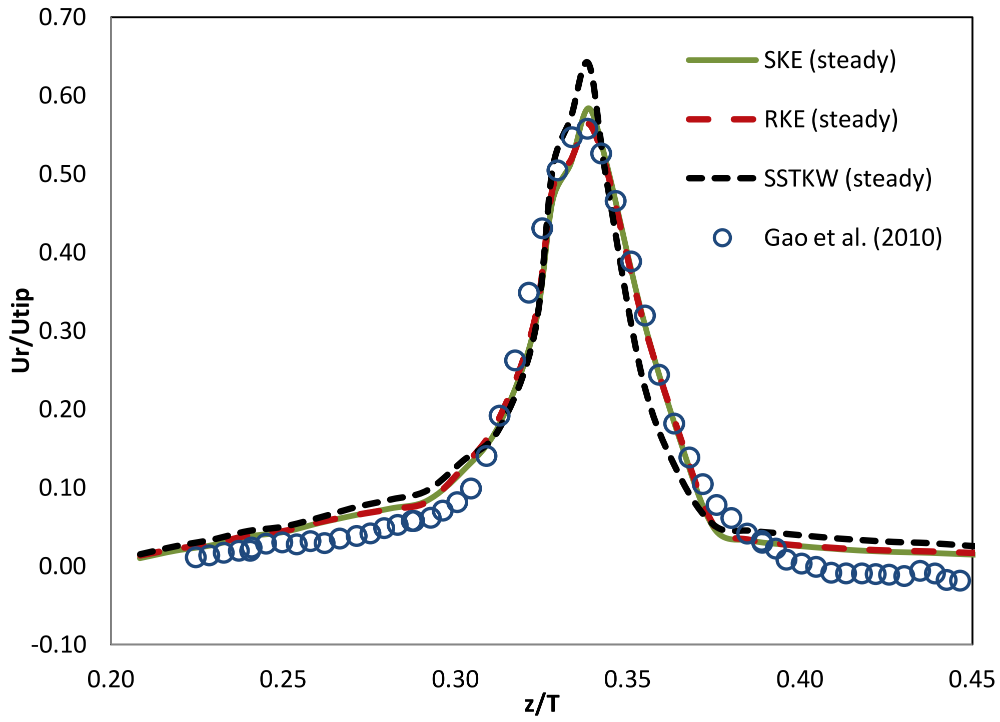

(a) Radial Velocity

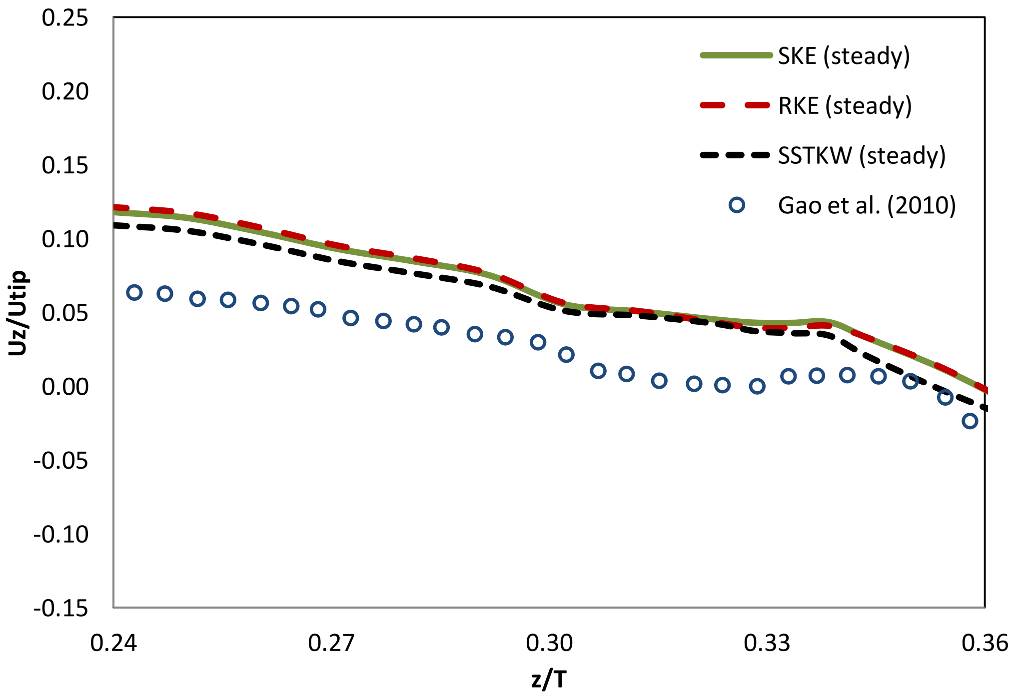

(b) Axial Velocity

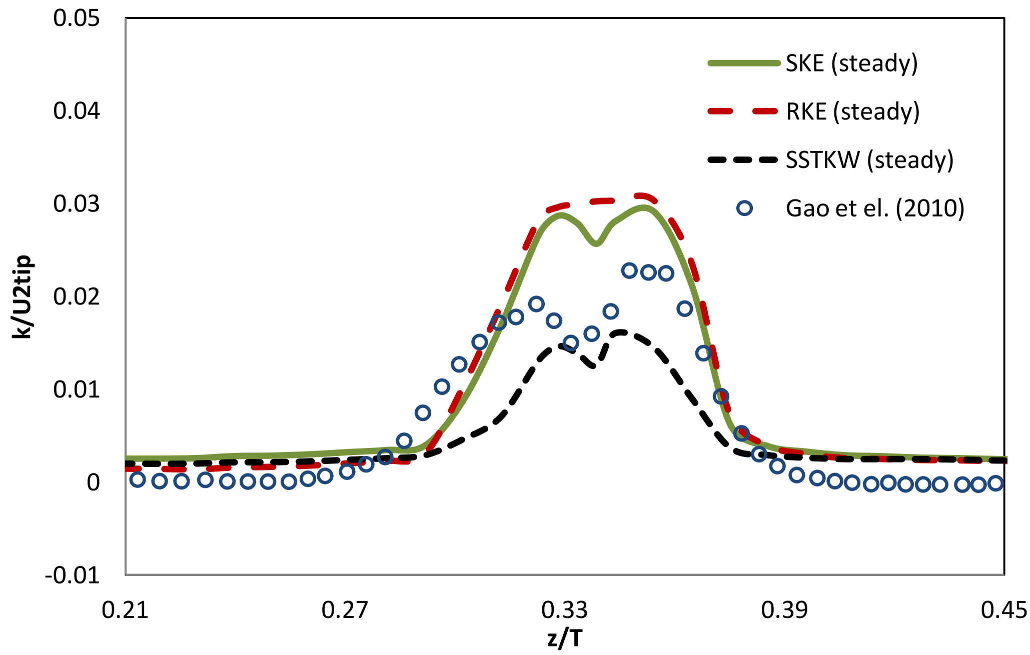

(c) Axial distributions of random turbulent kinetic energy

Figure 4.3 Comparison of different turbulence model at r/T= 0.245 of (a) Radial Velocity (b) Axial Velocity (c) Axial distributions of random turbulent kinetic energy

From figure 4.3, standard *k-ε* model, realizable *k-ε* model and shear-stress-transport *k-ω* model have similar trend which agree experimental data at the location above the impeller for radial and axial velocity profiles. But, in case of shear-stress-transport *k-ω* model, there is slightly deviation on radial velocity profiles. For random turbulent kinetic energy, the magnitudes of the random turbulent kinetic energy were over-predicted by standard *k-ε* model and realizable *k-ε* model even though the trends of variations and the locations of its maximum values were predicted well. Unlike for shear-stress-transport *k-ω* model, the magnitudes of the random turbulent kinetic energy and trends were located below the experimental data. Since low Reynolds number modeling was used (Re = 8847), realizable *k-ε* model and shear-stress-transport *k-ω* model was more practical than standard *k-ε* model which more suitable for simulation with high Reynolds number. Instead of using shear-stress-transport *k-ω* model, realizable *k-ε* model was used for the remaining of this work as it capabilities of predicting accurate mean flow distributions of velocity.

4.1.4 Comparison between Steady and Unsteady Simulation

In the past, most CFD perform using steady solver. Turbulent flows are unsteady by definition but it can be statically stationary. Steady flows are more tractable than unsteady flows. Nevertheless, steady computations produce an erroneously long wake because they omit an important component of the averaged flow field, the periodic vortex shading while unsteady flow represent real measurement. Experimental measurement is often taken as time averaged quantities and the unsteady solver mimics this situation better.

The realizable k-e turbulent model was employ to stimulate the stirred tank with HEDT similar to those studied by Gao et al. (2010).

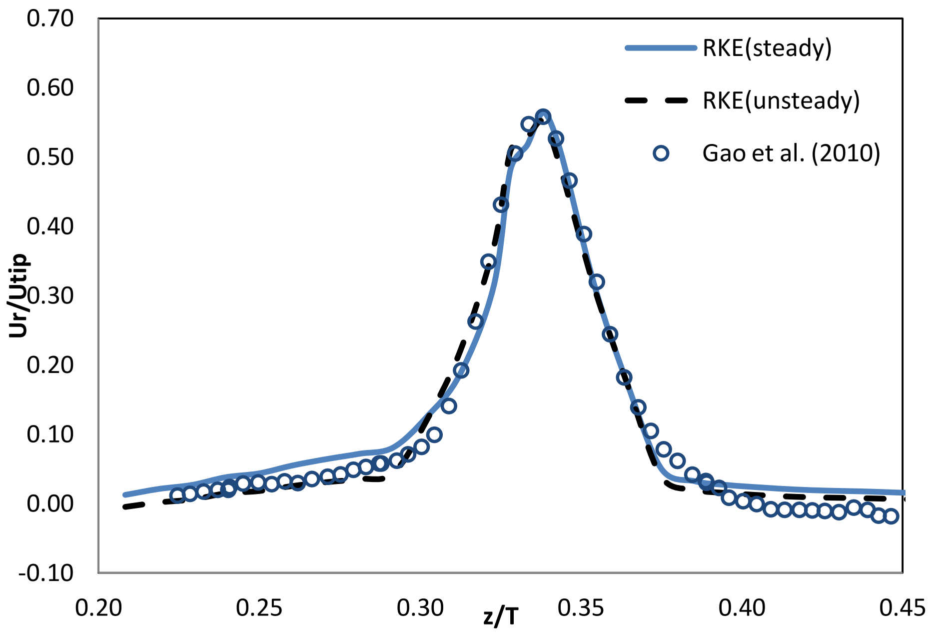

(a) Radial Velocity

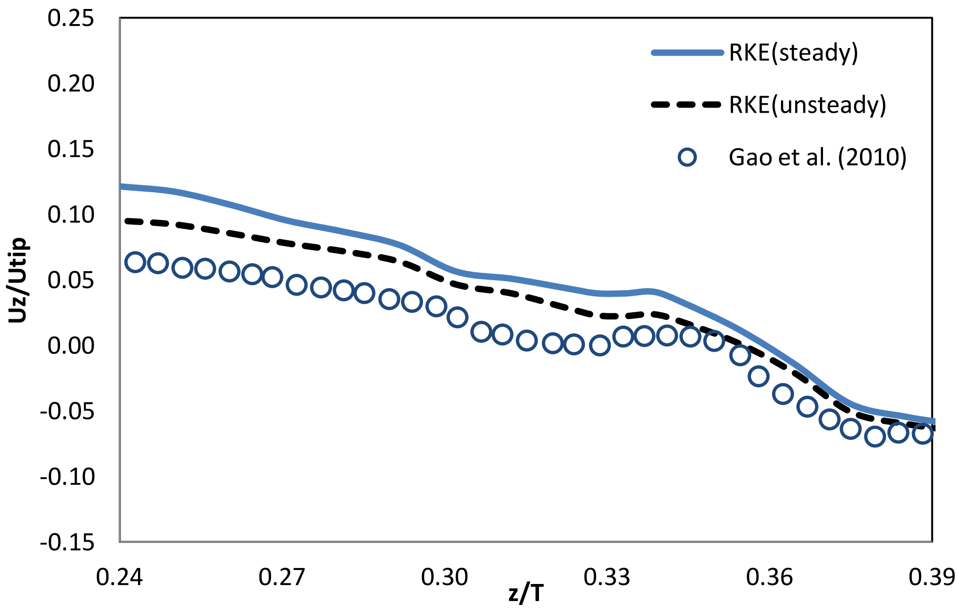

(b) Axial Velocity.

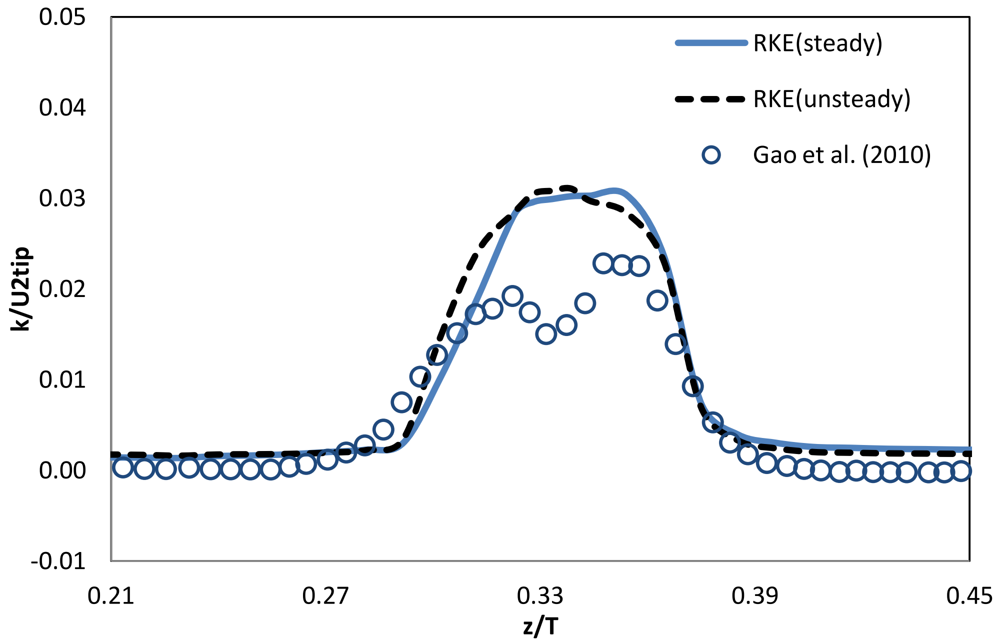

(c) Axial distributions of random turbulent kinetic energy

Figure 4.4 Comparison of experimental and computational predictions for steady and time average unsteady techniques at r/T=0.245 of (a) Radial Velocity (b) Axial Velocity (c) Axial distributions of random turbulent kinetic energy

Figure 4.4 shows a good agreement of the prediction of radial velocity, axial velocity and random turbulent kinetic energy for both the steady and unsteady solver with experimental data. As the flow is unsteady, realizable k-ε model averaging is not synonymous with time-averaging like steady flow. Hence, the simulation must be time dependent. Despite the time dependence, and large vertical structures, unsteady solver is a simulation of its statistics. One of the challenges to the numerical simulation of the flow in a stirred vessel is to simulate the fluid turbulence. Even though realizable k-ε model unable to resolve the two peaks exist in the impeller stream for random turbulent kinetic energy, the predictions were the most approaching the experimental data. Therefore, predictions of unsteady solver are much better than steady solver. According to Laccarino et al. (2003), the present study demonstrates that unsteady RANS does indeed predict periodic shedding, and leads to much better concurrence with available experimental data than has been achieved with steady computation.

4.2 SUMMARY

Second order scheme was used in this work as it is more accurate than first order upwind scheme. It is assumed that the gradient between the present node and the eastern face is the same as between downwind node and the present node.

The very coarse grid with 807 k cells and 1016k cells has minimal differences as the fine grid (1066k, 1100k and 1333k). However, improvement on prediction accuracy can be observed when the mesh density at 1066k as this grid is selective adaptive. Therefore, the intermediate grid with 1066k cells was chosen for the remainder of this work in interest to minimize the computational time.

Since low Reynolds number modeling was used, realizable *k-ε* model and shear-stress transport *k-ϖ* model was more practical than standard *k-ε* model which more suitable for simulation with high Reynolds number. Instead of using shear-stress transport *k-ϖ* model, realizable *k-ε* model was used for the remaining of this work as it capabilities of predicting accurate mean flow distributions of velocity. Since initial studies have shown that the realizable *k-ε* model provides the best performance of all the *k-ε* model versions for several validations of separated flows and flows with complex secondary flow features, realizable *k-ε* model had shown a better choice of turbulence model even as a relatively new model.

Unsteady solver indeed predicts periodic shedding, and leads to much better concurrence with available experimental data than has been achieved with steady computation. As the flow is unsteady, realizable *k-ε* model averaging is not synonymous with time-averaging like steady flow. Hence, the simulation must be time dependent. Despite the time dependence, and large vertical structures, unsteady solver is a simulation of its statistics.

CHAPTER 5

CONCLUSION AND RECOMMENDATION

5.1 CONCLUSIONS

In this study, Computational Fluid Dynamics (CFD) have been applied to achieved advance gas dispersion using deep hollow blade turbine (HEDT) as the impeller for single phase.

The second order discretisation scheme improves the prediction of flow features. The sliding mesh approach generally performs better in predicting the power number and flow numbers than the MRF approach, however, it requires a much longer computing time. Therefore, from an engineering standpoint, the MRF approach is recommended. MRF used to capture flow features in details and predicts flow for steady state for the impeller blades relative to the tank baffles.

From the three turbulence models (standard k-ε, realizable k-ε and shear-stress transport k-ϖ) used to predict flow distributions of velocity and turbulent kinetics energy, the realizable k-ε model is highly recommended.

Unsteady solver indeed predicts periodic shedding, and leads to much better concurrence with available experimental data than has been achieved with steady computation. Despite the time dependence, and large vertical structures, simulation of its statistics of unsteady solver is better than time-average independent of steady solver.

5.2 RECOMMENDATION

Since fluid dynamics of flow in stirred tank is extremely complex, the further investigation will focus on the effect of turbulence model for high Reynolds number. One of the ways to simulate turbulent flow in a stirred vessel is to perform large eddy simulation (LES) but simulation of a very high Reynolds number (typically 50,000 and higher) as encountered in practical applications require computational resources are expensive.

REFERENCES

Ansys Fluent 12.0. Theory Guide. 2009.

Aubin, J., Fletcher, D. F. and Xuereb, C. 2004. Modeling turbulent flow in stirred tanks with CFD: the influence of the modeling approach, turbulence model and numerical scheme. *Exp Therm Fluid Sci*. 28: 431-445.

Alcamo, R., Micale, G., Grisafi, F., Brucato, A. and Ciofalo, M. 2005. Large-eddy simulation of turbulent flow in an unbaffled stirred tank driven by a Rushton turbine. *Chemical Engineering Science.* 60(8)2303-2316.

Bao, Y., Gao, Z., Li, Z., Bai, D., Smith, J.M. and Thorpe, R.B. 2008. Solid Suspension in a Boiling Stirred Tank with Radial Flow Turbines. *Ind. Eng. Chem. Res,* 47, 2420-2427

Cooke, M. and Heggs, P.J. 2005. Advantages of the Hollow (Concave) Turbine for Multi-phase Agitation under Intense Operating Conditions. *Chemical Engineering Scienc.,* 60, 5529-5543.

Eggels, J. G.M. 1996. Direct and large eddy simulation of turbulent fluid flow using the lattice-Boltzmann scheme. *Int J Heat Fluid Flow.* 17(3):307-23.

Fluent 6.2. User Guide. 2005.

Fluent 6.2. User Guide. 2006.

Gimbun, J., Rielly, C.D. and Nagy,Z.K. 2009. Modelling of mass transfer in gas–liquid stirred tanks agitated by Rushton turbine and CD-6 impeller: A scale-up study. *Chemical Engineering Research and Design*. 87(4)437-451.

Gosling, I. 2005. *Process Simulation and Modelling for Industrial Bioprocessing. Industrial Biotechnology*. Ph.D. Thesis. GEN Publishing Inc.

Haiyan, S., Zhai-Shai, M. and Gengzhi, Y. 2006. Experimental and Numerical Study of Gas Hold-up in Surface Aerated Stirred Tanks. *Chemical Engineering Science.* 61, 4098-4110.

Hartmann, H., Derksen, J. J., Montavon, C., Pearson, J., Hamill, I. S. and van den Akker HEA. 2004. Assessment of large eddy and RANS stirred tank simulations by means of LDA. *Chemical Engineering Science*. 59: 2419-848.

Jahoda, M., Tomaskova, L. and Mostek, M. 2009. CFD prediction of liquid homogenisation in a gas-liquid stirred tank. *Chemical Engineering Research and Design*. 231- 238.

Jaworski, Z. and Dudczak, J. 1998. CFD modelling of turbulent macromixing in stirred tanks. Effect of the profile size and number of mixing indicates. *Compt Chem Eng*. 22(Suppl. 1):298-8.

Jaworski, Z. and Zakrzewska, B. 2002. Modelling of the turbulent wall jet generated by a pitched blade turbine impeller: the effect of turbulence model. *Chem. Eng. Res. Des*. 80:846-854.

Khopkar, A. R., Kasat, G. R., Pandit, A. B. and Ranade, V. V. 2006. CFD Simulation of Mixing in Tall Gas-Liquid Stirred Vessel: Role of Local Flow Patterns. *Chemical Engineering Science.* 61, 2921-2929.

Kshatriya, S.S., Patwardhan, A.W. and Eaglesham, A. 2007. Experimental and CFD Characterization of Gas Dispersing Asymmetric Parabolic Blade Impellers. *International Journal of Chemical Reactor Engineering.* 5, A12.

Laccarino, G., Ooi, A., Durbin, P.A. and Behnia, M. 2003. Reynolds averaged simulation of unsteady separated flow. *International Journal of Heat and Fluid Flow.* 24, 147-156.

Launder, B. E. and Spalding, D. B. 1972. *Lectures in Mathematical Models of Turbulence.* Academic Press, London, England.

Liu, X., Bao, Y., Li, Z. and Gao, Z. 2010. Analysis of Turbulence Structure in the Stirred Tank with Deep Hollow Blade Turbine by Time-Resolved PIV. *Chinese Journal of Chemical Engineering*. 18(4), 588-599.

Li, M., White, G., Wilkinson, D. and Roberts, K. J. 2005. Scale up study of retreat curve impeller stirred tanks using LDA measurements and CFD simulation. *Chemical Engineering Journal*. 108, 81-90.

Luo, J.Y., Issa, R. I. and Gosman, D. 1994. Prediction of impeller induced flows in mixing vessels using multiple frames of reference. *Icheme Symp Ser*.136:549.

Menter, F. R. 1994. Two-equation eddy-viscosity turbulence models for engineering applications. *AIAA Journal*. 32(8), 1598-1605.

Mostek, M., Kukukova, A., Jahoda, M. and Machon, V. 2005. Comparison of different techniques for modelling of flow field and homogenization in stirred vessels. Chemical Pap. 59 (6);380-5.

Murthy, B. N. and Joshi, J.B. 2008. Assessment of standard k-ε, RSM and LES turbulence models in a baffled stirred vessel agitated by various impeller designs. *Chemical Engineering Science.* 63, 5468-5495.

Murthy, J. Y. and Mathur, S. R. 1994. CFD simulation of flows in stirred tank reactors using a sliding mesh technique. *Icheme Symp Ser*. 136:341-8.

Myers, K. J., Thomas, A. J. and Bakker, A. 1999. Performance of a Gas Dispersion Impeller with Vertically Assymmetric Blades. *Institution of Chemical Engineers Trans Icheme.* 77, 1-3.

Ranade, V.V., Bourne, J.R. and Joshi, J.B.1991. Fluid mechanics and blending in agitated tanks. *Chemical Eng Science*. 46, 1883-93.

Revstedt, J., Fuchs, L. and Tradgardh, C. 1998. Large eddy simulations of the turbulent flow in a stirred reactor. *Chem Eng Sci*. 53(24):4041-53.

Scargiali, F., D'Orazio, A., Grisafi, F. and Brucato, A. 2007. Modelling and Simulation of Gas-Liquid Hydrodynamics in Mechanically Stirred Tanks. *Chemical Engineering Research and Design.* 85(A5), 637-646.

Shih,T.-H., Liou, W. W., Shabbir, A., Yang, Z. and Zhu, J. 1995. A new k-ε viscosity model for high Reynolds number turbulent flows – model development and validation. *Computers Fluid*. 24(3), 227-238.

Singh, H., Fletcher, D. F. and Nijdam, J. J. 2011. An assessment of different turbulence models for predicting flow in a baffled tank stirred with a Rushton turbine. *Chemical Engineering Science*. 66(23) 5976-5988.

Smith, J. M. and Gao, Z. 2001. Power Demand of Gas Dispersing Impellers Under High Load Conditions. *Institute of Chemical Engineers Trans Icheme*. 79, 1-6.

Vlaev, S.D., Mavros, P., Seichter, P. and Mann, R. 2002. Operational Characteristics of A New Energy- Saving Impeller for Gas-Liquid Mixing. *The Canadian Journal of Chemical Engineering.* 80,1-7.

Wang, W., Mao, Z-S. and Yang, C. 2006. Experimental and Numerical Investigation on Gas Holdup and Flooding in an Aerated Stirred Tank with Rushton Impeller. *Ind. Eng. Chem. Res.* 45, 1141-1151.

Wu, B. 2011. CFD investigation of turbulence models for mechanical agitation of non-Newtonian fluids in anaerobic digesters. *Water Research*. 45(5)Pages 2082-2094.

Yeoh, S.L., Papadakis, G. and Yianneskis, M. 2004. Numerical simulation of turbulent flow parameters in a stirred vessel using the LES and RANS approaches with the sliding /deforming mesh methodology. *Trans Icheme Part A Chem Eng Res Des*.82, 834-48.

Zadghaffari, R., Moghaddas, J.S. and Revstedt, J. 2010. Large-eddy simulation of turbulent flow in a stirredtank driven by a Rushton turbine. *Computers & Fluids.* 39: 1183-1190.

Zhao, J., Gao, Z. and Bao, Y. 2011. Effects of the Blade Shape on the Trailing Vortices in Liquid Flow Generated by Disc Turbines. *Chinese Journal of Chemical Engineering.* 19(2)232-242.